Scaling of the magnetic entropy change in skyrmion material $Fe_{0.5}Co_{0.5}Si$

Hui Han,[1,2] Dirk Menzel,[3] Wei Liu,[1,2] Langsheng Ling,[1] Haifeng Du,[1] Li Pi,[1,4] Changjin Zhang,[1] Lei Zhang,[1,*] and Yuheng Zhang[1,4]

[1] *Anhui Key Laboratory of Condensed Matter Physics at Extreme Conditions, High Magnetic Field Laboratory, Chinese Academy of Sciences, Hefei 230031, China*

[2] *University of Science and Technology of China, Hefei 230026, China*

[3] *Institut für Physik der Kondensierten Materie, Technische Universität Braunschweig, D-38106 Braunschweig, Germany*

[4] *Hefei National Laboratory for Physical Sciences at the Microscale, University of Science and Technology of China, Hefei 230026, China*

(Dated: June 25, 2017)

Abstract

The magnetic entropy change $[\Delta S_M(T,H)]$ around the phase transition temperature T_C is investigated by the scaling method for $Fe_{0.5}Co_{0.5}Si$, which exhibits a skyrmion phase below T_C. The parameters of $\Delta S_M(T,H)$ exhibit field dependent behaviors. The $\Delta S_M(T,H)$ curves under high field can be well scaled into a single universal curve independent of external field and temperature. However, $\Delta S_M(T,H)$ curves under low field become divergent just below T_C, which indicates a characteristic of first-order transition. The scaling investigation of $\Delta S_M(T,H)$ curves indicates that the phase transition in $Fe_{0.5}Co_{0.5}Si$ is of a weak first-order type in low field region, while it is driven into a second-order one under high field. This weak first-order phase transition in low field region resembles that in typical skyrmion system MnSi which is caused by the critical fluctuation. The result suggests that critical fluctuation plays an important role in the phase transition and formation of skyrmion state.

PACS numbers: 75.30.Sg, 75.40.-s, 75.40.Cx

Keywords: magnetic entropy change; scaling; first-order phase transition; universal curve

*Corresponding author. Email:zhanglei@hmfl.ac.cn

I. INTRODUCTION

The chiral magnetic materials have attracted much attention recently due to the exotic physical phenomena, such as magnetic quantum phase transition, anomalous Hall effect, non-Fermi liquid behavior, and tricritical point [1–4]. These fascinating phenomena originate from the competition and balance between the spin, orbital, charge, and lattice degrees of freedom. In B20 compounds belonging to the $P2_13$ space group, due to the noncentrosymmetric structure, the lack of inversion symmetry usually results in the Dzyaloshinsky-Moriya (DM) interaction, which is 1∼2 orders of magnitude smaller than the ferromagnetic coupling [5]. The competition between DM spin-orbital coupling and strong ferromagnetic exchange usually generates a helical magnetic ordering with long-wave length modulation [6–8]. The helical magnetic ground state can be polarized into conical ordering by the external field [9]. When an appropriate external magnetic field is applied, a skyrmion state, which is a topologically stable vortex-like spin texture with nano-size, appears at the boundaries between the conical ordering and paramagnetic phases just below T_C [9, 10]. The B20 compounds, such as $Fe_{1-x}Co_xSi$, FeGe, MnSi with the cubic cell, are typical systems to investigate the chirality of the spin helix and the quantum phase transitions [11–14].

In the chiral magnetic systems, $Fe_{1-x}Co_xSi$ has been prominent for its easy modulation through the doping of Co [14, 15]. As we know, FeSi is paramagnetic with a strongly correlated narrow gap while CoSi is a diamagnetic metal [16]. However, $Fe_{1-x}Co_xSi$ exhibits itinerant magnetic properties [17, 18]. In addition, the magnetic helical ordering in $Fe_{1-x}Co_xSi$ can be changed from the right-handed to left-handed tuned by the content of Co [19]. The spin-interaction can also be modulated by the doping of Co [20]. It has been demonstrated that the change of magnetic chirality and spin interaction by doping are due to the tune of the DM interaction [15]. Especially, the half-doped $Fe_{0.5}Co_{0.5}Si$ exhibits complex non-collinear magnetic ordering and precursor phenomena [13, 21]. Therefore, the investigation of $Fe_{0.5}Co_{0.5}Si$ is of great importance to uncover the magnetic interaction of this system.

As we know, the magnetic entropy changes when the phase transition occurs, which is an effective means to study the magnetic interaction [22–25]. In this work, we perform a scaling investigation of the magnetic entropy change around the phase transition temperature for $Fe_{0.5}Co_{0.5}Si$. The scaling investigation of the magnetic entropy change suggests that the

phase transition in $Fe_{0.5}Co_{0.5}Si$ exhibits a weak first-order characteristic under low field, which is driven into a second-order one by high magnetic field.

II. EXPERIMENT

A single crystal sample of $Fe_{0.5}Co_{0.5}Si$ was prepared by the Czochralski method [26]. The physical properties were checked in elsewhere [20]. The magnetization measurement was performed by using a Quantum Design Vibrating Sample Magnetometer (SQUID-VSM). The initial isothermal magnetization around the phase transition temperature (T_C) were recorded to calculate the magnetic entropy change. Before the data collection, the magnetic field was swept to zero in an oscillating mode. Then, the temperature was warmed to 100 K ($T \gg T_C$) waiting for two minutes. Then the temperature is decreased to the target temperature. After waiting for two minutes, the no-overshoot mode was applied to get a precise magnetic field. For the measurement of each initial magnetization curve, the magnetic field is decreased to zero field in the oscillating mode to remove the remained field. Each initial isothermal magnetization curve was measured in the same procedure to ensure a precise magnetic field and temperature.

III. RESULTS AND DISCUSSION

Figure 1 (a) shows the temperature dependence of magnetization [$M(T)$] (left axis) for $Fe_{0.5}Co_{0.5}Si$ under zero-field-cooling (ZFC) and field-cooling (FC) sequences with an applied field $H = 10$ Oe. The magnetic transition temperature T_C is determined from the peak of $M(T)$ curve as $T_C \sim 44$ K. The temperature dependence of reciprocal susceptibility [$\chi^{-1}(T) = (M/H)^{-1}$] curve is also given in Fig. 1 (a) (right axis). The $\chi^{-1}(T)$ curve exhibits a straight linear behavior above T_C, which indicates a paramagnetic behavior. The $\chi^{-1}(T)$ obeys the Curie-Weiss law: $\chi(T) = C/(T - \theta_{CW})$, where $C = 0.0467(9)$ [emu K/g Oe] is the Curie constant, and $\theta_{CW} = 49.12(6)$ K is the Curie-Weiss temperature. The inset of Fig. 1 (a) plots the isothermal magnetization [$M(H)$] at 4 K, which displays a typical magnetic ordering behavior with no magnetic hysteresis. In order to generate the magnetic entropy change, the initial $M(H)$ curves in the vicinity of T_C are given in Figure 1 (b). The inset of Fig. 1 (b) gives the $M(H)$ curve in the low field region at 20 K, which shows that

saturate magnetic field $H_S \sim 500$ Oe.

Based on the thermodynamical theory, the magnetic entropy change $[\Delta S_M(T,H)]$ induced by the external field is given by: [27]:

$$\Delta S_M(T,H) = \int_0^{H^{max}} \left[\frac{\partial S(T,H)}{\partial H}\right]_T dH \tag{1}$$

with the Maxwell's relation $[\partial S(T,H)/\partial H]_T = [\partial M(T,H)/\partial T]_H$, $\Delta S_M(T,H)$ is written as [28]:

$$\Delta S_M(T,H) = S_M(T,H) - S_M(T,0) = \int_0^{H^{max}} \left[\frac{\partial M(T,H)}{\partial T}\right]_H dH \tag{2}$$

where H is the external magnetic field, T is the temperature, and H^{max} is the maximum of external magnetic field. Based on the initial $M(H)$ curves in Fig. 1 (b), the temperature dependence of ΔS_M $[-\Delta S_M(T)]$ curves under different H are calculated. Figure 2 (a) and (b) show the $-\Delta S_M(T)$ curves around T_C under high and low field, respectively. For each $-\Delta S_M(T)$ curve under selected field, a peak appears around T_C. The position of the peak shifts slightly to the higher temperature direction with the increase of H, with the temperature offset $\Delta T \sim 2$ K. The value of $-\Delta S_M(T)$ almost decreases symmetrically on both sides. The magnitude of each $-\Delta S_M(T)$ curve for the fixed temperature increases with the applied magnetic field and reaches at the maximum value of 0.74 J/(kg·K) when $H = 30$ kOe.

The shape of $-\Delta S_M(T)$ curve changes as the increase of field, such as the broadening and increase of the curves. The change of $-\Delta S_M(T)$ vs. H can be quantified by the parameters, which usually follows power laws as a function of field. Figure 3 (a), (b), and (c) show the field dependence of parameters of $|\Delta S_M^{max}|$ (the maximum of the magnetic entropy change), δ_{FWHM} (the full width at half maximum), and $RCP(S)$ (the relative cooling power), respectively. It can be seen that all parameters of $|\Delta S_M^{max}|$, δ_{FWHM}, and $RCP(S)$ are field dependent, which obey the relations as [29]:

$$\begin{cases} |\Delta S_M^{max}(T)| \propto H^n \\ \delta_{FWHM} \propto H^b \\ RCP(S) \propto H^c \end{cases} \tag{3}$$

where n, b, and c are exponents related to the magnetism of the system. For $|\Delta S_M^{max}|$ vs. H, it can be obtained that $n = 0.7431(2)$. Previous investigations on different soft magnetic amorphous alloys have demonstrated that n is close to 1 well below T_C while it approaches

2 well above T_C [30]. However, n exhibits a complex behavior around T_C, which is related to the critical behavior. Based on the Landau mean field theory, n should be equal to 2/3 at T_C. However, for a typical soft magnetic amorphous alloy, $n \sim 0.75$ around T_C [30]. The obtained $n = 0.7431(2)$ for $Fe_{0.5}Co_{0.5}Si$ is very close to that of soft magnetic amorphous alloy, which is also confirmed by no magnetic hysteresis phenomenon on $M(H)$ curve. The δ_{FWHM} implies the broadening of $-\Delta S_M(T)$ curves with the increase of H, as shown in Fig. 3 (b). The fitting of the δ_{FWHM} vs. H gives that $b = 0.3817(6)$. The $RCP(S)$ is defined as [30, 31]:

$$RCP(S) = |\Delta S_M^{max} \times \delta_{FWHM}| \tag{4}$$

The fitting of $RCP(S)$ vs. H in Fig. 3 (c) yields that $c = 1.1034(4)$.

The variation of the phase transition can be also demonstrated by the magnetic specific heat change $[\Delta C_P(T, H)]$. The $\Delta C_P(T, H)$ is obtained from the change of $\Delta S_M(T, H)$ as [32]:

$$\Delta C_p(T, H) = C_p(T, H) - C_p(T, 0) = T\frac{\partial \Delta S_M(T, H)}{\partial T} \tag{5}$$

The temperature dependence of $-\Delta C_P$ under different H is depicted in Fig. 4. The $-\Delta C_P$ changes from positive for $T > T_C$ to negative for $T < T_C$ with temperature decreasing, which corresponds to paramagnetic to magnetic ordering phase transition. The magnetic transition temperature can be determined by temperature corresponding to the zero point of ΔC_P $[\Delta C_P(T, H)|_{T_C} = 0]$. However, it can be seen that T_C exhibits a fluctuation of $\Delta T \sim 2$ K, which is in agreement with the peak shift of $\Delta S_M(T, H)$ in Fig. 2.

The field dependence of magnetic entropy change $[-\Delta S_M(H)]$ at different temperatures are depicted in Fig. 5 (a) and (b). The magnetic entropy change increases monotonically with the increase of external magnetic field. Figure 5 (a) and (b) depict the $[-\Delta S_M(H)]$ above and below T_C, respectively. The maximum value of $-\Delta S_M(T)$ appears around 46 K as shown in Fig. 5 (a). The value n can be calculated by [33]:

$$n(T, H) = \frac{d\ln(|\Delta S_M(T, H)|)}{d\ln(H)} \tag{6}$$

Figure 5 (c) and (d) show the temperature dependence of n under high and low field based on Fig. 5 (a) and (b). The n vs. T $[n(T)]$ curve under high field is raised with the increase of field as shown in Fig. 5 (c), where n reaches the minimum value around T_C. However, $n(T)$ curves under low field become divergent, as shown Fig. 5 (d). Generally, the divergence

of the $n(T)$ implies a first-order phase transition [34, 35]. The type of the phase transition should be firmly testified by the scaling of $\Delta S_M(T,H)$ curves.

The $-\Delta S_M(T,H)$ curves can be investigated by the scaling method based on the critical phenomenon [29–31]. According to scaling laws, the experimental $-\Delta S_M(T,H)$ should collapse onto two independent universal curves below and above T_C with proper reference temperatures and normalization. The $-\Delta S_M(T,H)$ is normalized by $\Delta S'_M = |\Delta S_M(T)/\Delta S_M^{max}(T)|$, and the temperature is normalized by reference temperature T_r into a re-scaled temperature θ. The horizontal coordinate is marked as the re-scaled temperature θ, which is defined as [29]:

$$\theta = \frac{T - T_C}{T_r - T_C} \tag{7}$$

By choosing proper T_r, the equivalent points of the different experimental curves should collapse onto the same point on the universal curve [29]. The experimental $\Delta S'_M$ should collapse onto two independent universal curves below and above T_C respectively. The combination of the two universal curves below and above T_C just form a whole universal magnetic entropy change curve. After scaling and normalizing, T_r should locate at a value of $\theta = 1$ on the universal curve $[\Delta S'_M(\theta)]$. However, in multiple magnetic phases, the use of two reference temperatures is necessary. After normalizing the curves, T_{r1} and T_{r2} are just corresponding to $\theta = -1$ and $\theta = +1$ respectively. The re-scaled temperature θ is defined as [29]:

$$\theta = \begin{cases} \theta_- = (T_C - T)/(T_{r1} - T_C), T \leq T_C \\ \theta_+ = (T - T_C)/(T_{r2} - T_C), T > T_C \end{cases} \tag{8}$$

where T_{r1} and T_{r2} are the reference temperatures below and above T_C respectively, which corresponds to $\Delta S_M(T_{r1}, T_{r2}) = \frac{1}{2}\Delta S_M^{max}$. According to the scaling equation, the order of the magnetic phase transition can be judged by this scaling method. If the curves around T_C can be re-scaled into a single universal curve independent of H and T, the phase transition is of a second-order type [34]. Otherwise, the divergence of the re-scaled $\Delta S'_M(\theta)$ curves suggests a first-order one [22]. This method has already been extensively applied in many kinds of systems, such as MnSi, $Gd(Si_xGe_{1-x})_4$, and many Heusler alloys [23, 36–38].

The construction of a universal scaling of the experimental $-\Delta S_M(T,H)$ are plotted in Fig. 6. The $\Delta S_M(T)$ curves for different H were normalized as $\Delta S'_M$ on the longitudinal coordinate, where the maximum of all curves are located on single point. The temperature is plotted as θ. Figure 6 (a) and (b) depict the $\Delta S'_M(\theta)$ curves under high and low field,

respectively. In Fig. 6 (a), all experimental data collapse into a single universal curve, where T_{r1} and T_{r2} are field dependent as shown in the inset of Fig. 6 (a). The good convergence of the $\Delta S'_M(\theta)$ curves under high field indicates the magnetic transition is of the second-order type [22]. A universal curve can be fitted, which is independent of the external measurement conditions but just determined by the intrinsic magnetization. The n values at high field can also be scaled into $n(\theta)$ as shown in the inset of Fig. 5 (c), which confirms the scaling of $-\Delta S_M(T, H)$ curves at high field. However, in Fig. 6 (b), $\Delta S'_M(\theta)$ curves below 900 Oe cannot be scaled into a single curve. The $\Delta S'_M(\theta)$ curves becomes divergent just below T_C. The non-convergent behavior of the scaling curves of magnetic entropy change suggests a first-order phase transition under low field below 900Oe [22].

The scaling investigation of the magnetic entropy change in $Fe_{0.5}Co_{0.5}Si$ demonstrates that the magnetic transition exhibits a weak first-order characteristic under low field, while displays a second-order one in high field region. In other word, the external field drives the weak first-order magnetic transition into a second one. In fact, the small angle neutron scattering (SANS) experiment has also suggests that the phase transition in $Fe_{0.5}Co_{0.5}Si$ exhibits a weak first-order characteristic under zero field [39], which is in agreement with the result in this work. This field-driven phase transition is usually observed in the B20 compounds. In MnSi, which is a typical skyrmion system analogous to that in $Fe_{0.5}Co_{0.5}Si$, the first-order phase transition is also be driven into a second one by the external field [22, 40]. According to the Brazovskii scenario, the first-order phase transition from paramagnetic to helimagnetic ordering in the B20 compound is induced by the critical fluctuation under zero field, which can be suppressed by the external magnetic field [41]. Therefore, it is suggested that the first-order characteristic induced by critical fluctuation plays an important role in the phase transition and formation of skyrmion in $Fe_{0.5}Co_{0.5}Si$.

IV. CONCLUSION

In summary, we have performed scaling investigation of the magnetic entropy change around T_C in the B20 compound $Fe_{0.5}Co_{0.5}Si$. The parameters of $\Delta S_M(T, H)$ curves ($|\Delta S_M^{max}|$, δ_{FWHM}, and $RCP(S)$) depends on the field as power law behaviors. The $\Delta S_M(T, H)$ curves under high field above 1 kOe can be well scaled into a single universal curve $\Delta S'_M(\theta)$ independent of external field and temperature. However, $\Delta S'_M(\theta)$ curves

under low field below 900 Oe become divergent just below T_C, which indicates a characteristic of first-order transition. The scaling investigation of the magnetic entropy change suggests that the phase transition in $Fe_{0.5}Co_{0.5}Si$ is of a weak first-order type in low field region below 900 Oe, while it is driven into a second-order one under high field. This field-driven phase transition is analogous to that in MnSi, which is attributed to the critical fluctuation. The result suggests that the critical fluctuation plays an important role in the phase transition and formation of skyrmion in $Fe_{0.5}Co_{0.5}Si$

V. ACKNOWLEDGEMENTS

This work is supported by the Ministry of Science and Technology of China (Grant No.: 2017YFA0303200) and the National Natural Science Foundation of China (Grant Nos. 11574322, U1332140, 11474290, and 11574288).

[1] N. Manyala, Y. Sidis, J. F. DiTusa, G. Aeppli, D. P. Young, Z. Fisk, Nature (London) **404** (2000) 581.

[2] C. Pfleiderer, S. R. Julian, G. G. Lonzarich, Nature (London) **414,** (2001) 427.

[3] C. Pfleiderer, G. J. McMullan, S. R. Julian, G. G. Lonzarich, Phys. Rev. B **55** (1997) 8330.

[4] F. Jonietz, S. Muhlbauer, C. Pfleiderer, A. Neubauer, W. Munzer, A. Bauer, T. Adams, R. Georgii, P. Boni, R. A. Duine, K. Everschor, M. Garst, A. Rosch, Science **330** (2010) 1648.

[5] Y. Togawa, T. Koyama, K. Takayanagi, S. Mori, Y. Kousaka, J. Akimitsu, S. Nishihara, K. Inoue, A. S. Ovchinnikov, J. Kishine, Phys. Rev. Lett. **108** (2012) 107202.

[6] S. V. Grigoriev, N. M. Potapova, S. A. Siegfried, V. A. Dyadkin, E. V. Moskvin, V. Dmitriev, D. Menzel, C. D. Dewhurst, D. Chernyshov, R. A. Sadykov, L. N. Fomicheva, and A. V. Tsvyashchenko, Phys. Rev. Lett. **110** (2013) 207201.

[7] A. N. Bogdanov, D. A. Yablonskii. Sov. Phys. JETP 68, 101 (1989).

[8] U. K. Roβler, A. N. Bogdanov, C. Pfleiderer, Nature (London) **442** (2006) 797.

[9] S. Muuhlbauer, B. Binz, F. Jonietz, C. Pfleiderer, A. Rosch, A. Neubauer, R. Georgii, P. Boni, Science **323** (2009) 915.

[10] A. Fert, V. Cros, J. Sampaio, Nat. Nanotechnol. **8** (2013) 152.

[11] W. Munzer, A. Neubauer, T. Adams, S. Muhlbauer, C. Franz, F. Jonietz, R. Georgii, P. Boni, B. Pedersen,M. Schmidt, A. Rosch, C. Pfleiderer. Phys. Rev. B **81** (2010) 041203(R)

[12] X. Z. Yu, N. Kanazaw, Y. Onose, K. Kimoto, W. Z. Zhang, S. Ishiwata, Y. Matsui, Y. Tokura, Nat. Mater. **10** (2011) 106.

[13] X. Yu, Y. Onose, N. Kanazawa, J. Park, J. Han, Y. Matsui, N. Nagaosa, Y. Tokura, Nature (London) **465** (2010) 901.

[14] A. Bauer, M. Garst, C. Pfleiderer, Phys. Rev. Lett. **93** (2016) 235144.

[15] S. V. Grigoriev, D. Chernyshov, V. A. Dyadkin, V. Dmitriev, S. V. Maleyev, E. V. Moskvin, D. Menzel, J. Schoenes, H. Eckerlebe. Phys. Rev. Lett. **102** (2009) 037204.

[16] O. Delaire, I. I. Al-Qasir, A. F. May, C. W. Li, B. C. Sales, J. L. Niedziela, J. Ma, M. Matsuda, D. L. Abernathy, T. Berlijin, Phys. Rev. B, **91** (2015) 094307.

[17] V. V. Mazurenko, A. O. Shorikov, A. V. L ukoyanov, K.Kharlov, E. Gorelov, A. I. Lichtenstein, V. I. Anisimov, Phys. Rev. B **81** (2010) 125131.

[18] Y. Onose, N. Takeshita, C. Terakura, H. Takagi, Y. Tokura, Phys.Rev. B **72** (2005) 224431.

[19] S. A. Siegfried, E. V. Altynbaev, N. M. Chubova, V. Dyadkin, D. Chernyshov, E. V. Moskvin, D. Menzel, A. Heinemann, A. Schreyer, S. V. Grigoriev, Phys. Rev. B **91** (2015) 184406.

[20] L. Zhang, D. Menzel, H. Han, C. Jin, H. Du, J. Fan, M. Ge, L. Ling, C. Zhang, L. Pi, Y Zhang, EPL **115** (2016) 67006.

[21] A. Bauer, M. Garst, C. Pfleiderer, Phys. Rev. B **93** (2016) 235144.

[22] S. S. Samatham and V. Ganesan, Phys. Rev. B **95** (2017) 115118.

[23] M. Ge, L. Zhang, D. Menzel, H. Han, C. Jin, C. Zhang, L. Pi, Y. Zhang. J. Alloys Compd. **649** (2015) 46.

[24] L. Xu, H. Han, J. Fan, D. Shi, D. Hu, H. Du, L. Zhang, Y. Zhang, H. Yang, EPL **117** (2017) 47004.

[25] L. Xu, J. Fan, Y. Zhu, Y. Shi, L. Zhang, L. Pi, Y. Zhang, D. Shi, Mater. Res. Bull. **73** (2016) 187.

[26] A. M. Racu, D. Menzel, J. Schoenes, K. Doll, Phys. Rev. B **76** (2007) 115103.

[27] V. Pecharsky, K. Gscheidner, J. Magn. Magn. Mater. **200** (1999) 44.

[28] D. J. Griffiths, *Introduction to electrodynamics (Third ed.)*. Prentice Hall. pp. 559-562. (1999).

[29] V. Franco, A. Conde, Int. J. Refrigerat. **33** (2010) 465.

[30] V. Franco, J. S.Blazquez, A. Conde, Appl. Phys. Lett. **89** (2006) 222512.

[31] V. Franco, A. Conde, J. M. Romero-Enrique, J. S. Blazquez, J. Phys.: Condens. Matter **20** (2008) 285207.

[32] X. X. Zhang, G. H. Wen, F. W. Wang, W. H. Wang, C. H. Yu, G. H. Wu, Appl. Phys. Lett. **77** (2000) 3072.

[33] H. Han, L. Zhang, X. Zhu, H. Du, M. Ge, L. Ling, L. Pi, C. Zhang, Y. Zhang. J. Alloys Compd. **693** (2017) 389.

[34] C. Romero-Muniz, R. Tamura, S. Tanaka, V. Franco. Phys. Rev. B **94** (2016) 134401.

[35] C. Bonilla, J. Herrero-Albillos, F. Bartolome, L. Garcia, M. Parra-Borderias, V. Franco, Phys. Rev. B **81** 224424 (2010) 1.

[36] J. Fan, L. Ling, B. Hong, L. Pi, Y. Zhang, J. Magn. Magn. Mater. **321** (2009) 2838.

[37] E. P. Nobrega, N. A. Oliveira, P. J. Ranke, A. Troper, Phys. Rev. B **72**(2005) 134426.

[38] V. D. Buchelnikov, V. V. Sokolovskiy, H. C. Herper, H. Ebert, M. E. Gruner, S. V. Taskaev, V. V. Khovaylo, A. Hucht, A. Dannenberg, M. Ogura, H. Akai, M. Acet, P. Entel, Phys. Rev. B **81** (2010) 094411

[39] V. A .Dyadkin, S. V. Grigoriev, E. V. Moskvin , S. V. Maleyev, D. Menzel, J. Schoenes , H. Eckerlebe, Physical B **404** (2009) 2520.

[40] S. M. Stishov, A. E. Petrova, S. Khasanov, G. K. Panova, A. A. Shikov, J. C. Lashley, D. Wu, T. A. Lograsso. Phys. Rev. B **76** (2007) 052405.

[41] S. A. Brazovskii, Zh. Eksp. Teor. Fiz. **68** (1975) 175 [Sov. Phys. JETP **41** (1975) 85].

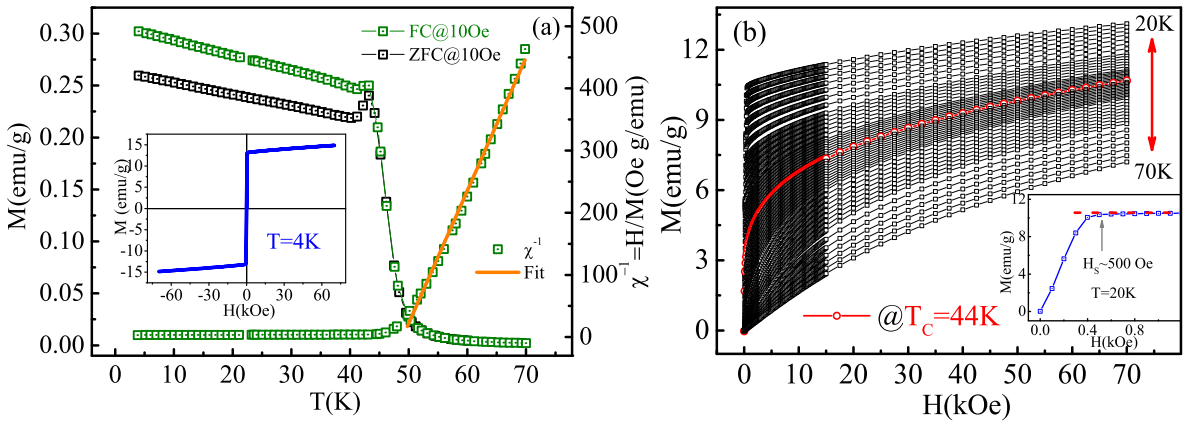

FIG. 1: (Color online) (a) Temperature dependence of magnetization $[M(T)]$ (left axis) and reciprocal susceptibility $[\chi^{-1(}T)]$ (right axis) under $H = 10$ Oe for $Fe_{0.5}Co_{0.5}Si$ (the inset shows the magnetization as a function of field $[M(H)]$ at 4K); (b) the initial isothermal $M(H)$ around T_C (the inset gives the one at 20 K in the low field region).

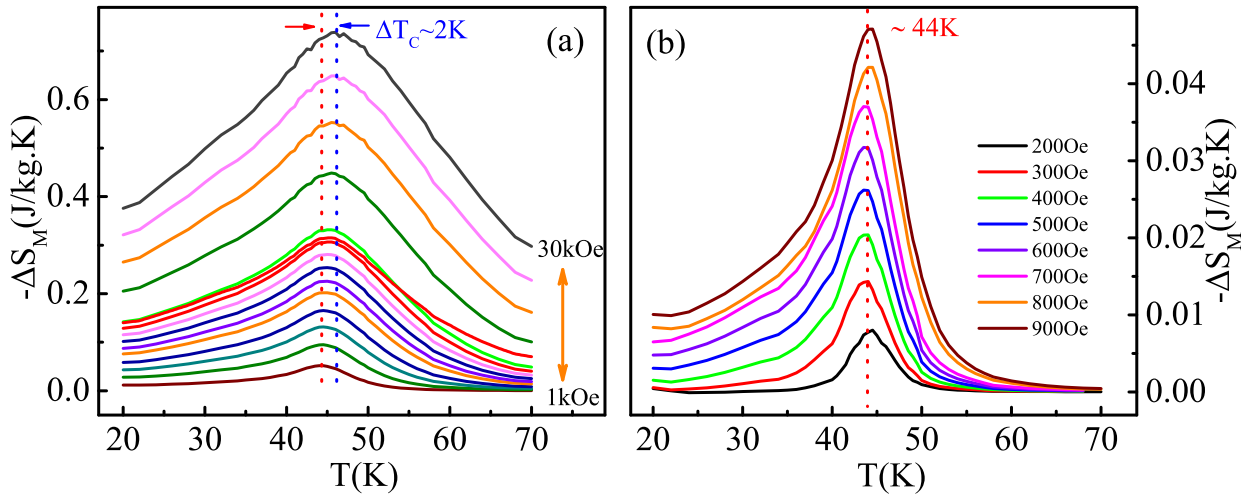

FIG. 2: (Color online) (a) Temperature dependence of $-\Delta S_M$ $[-\Delta S_M(T)]$ under different H in high field region; (b) $-\Delta S_M(T)$ curves under different H in low field region.

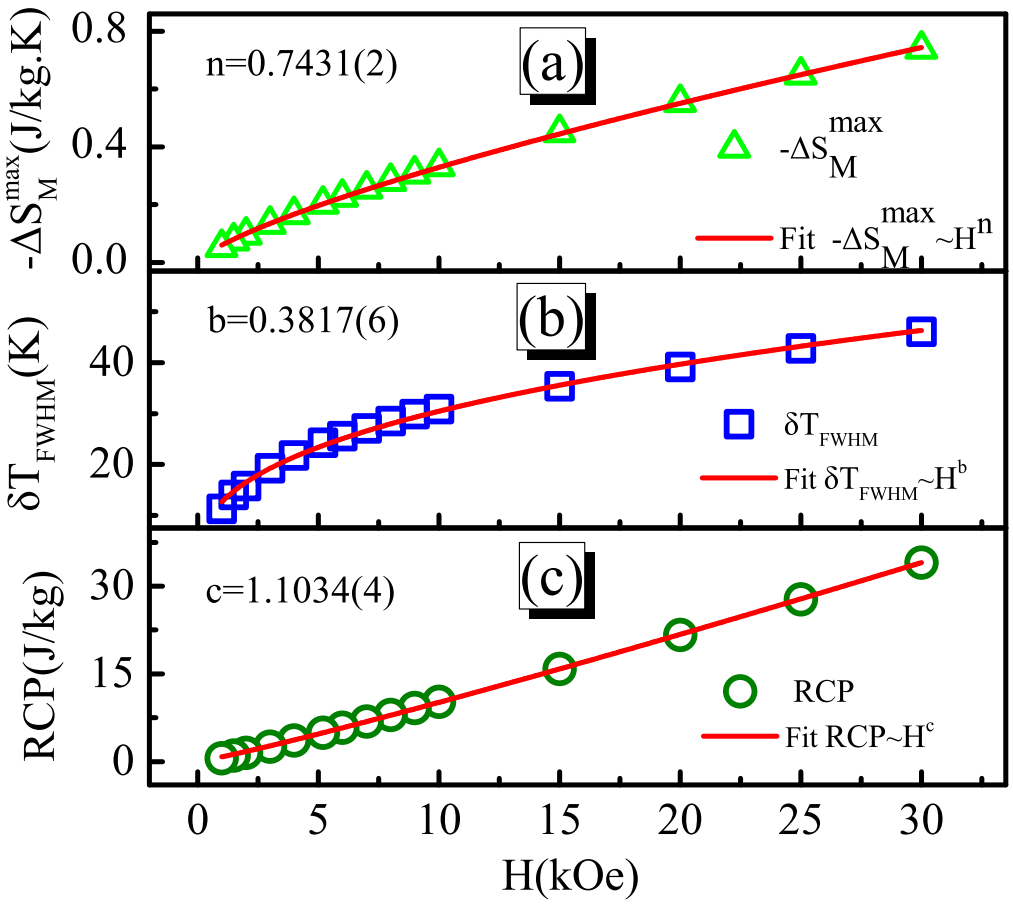

FIG. 3: (Color online) The field dependence of parameters of $-\Delta S_M(T,H)$ curves: (a) $-\Delta S_M^{max}$ vs. H, (b) δ_{FWHM} vs. H, and (c) $RCP(S)$ vs. H (red solid curves are fitted).

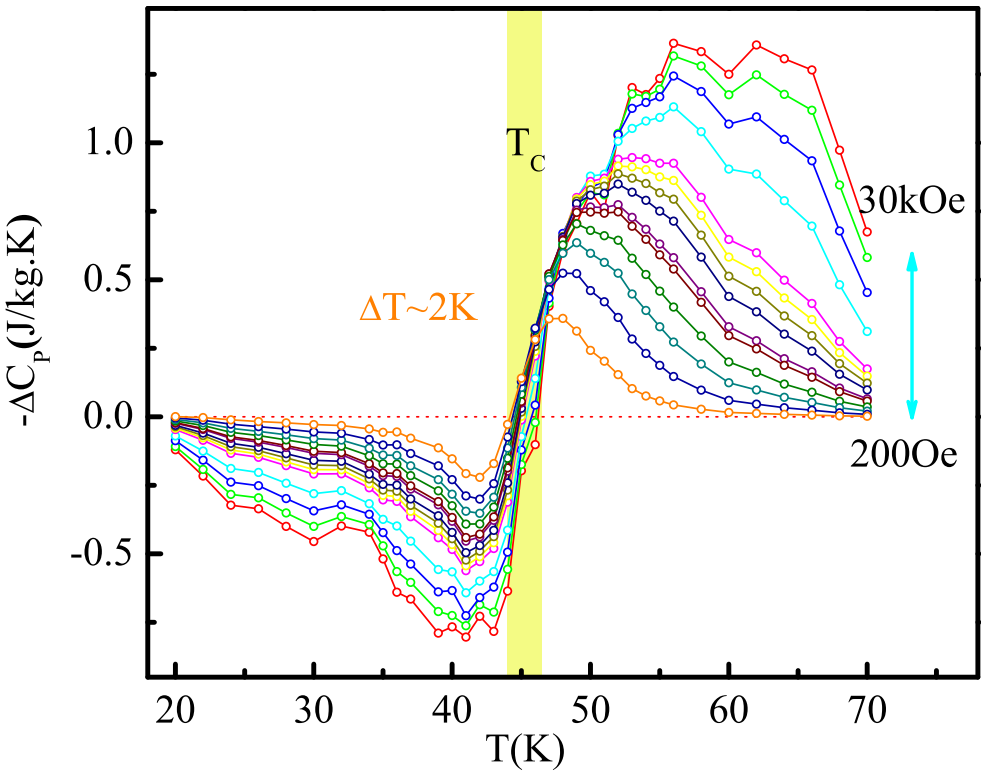

FIG. 4: (Color online) Temperature dependence of $-\Delta C_p$ $[-\Delta C_p(T)]$ under different H for $Fe_{0.5}Co_{0.5}Si$.

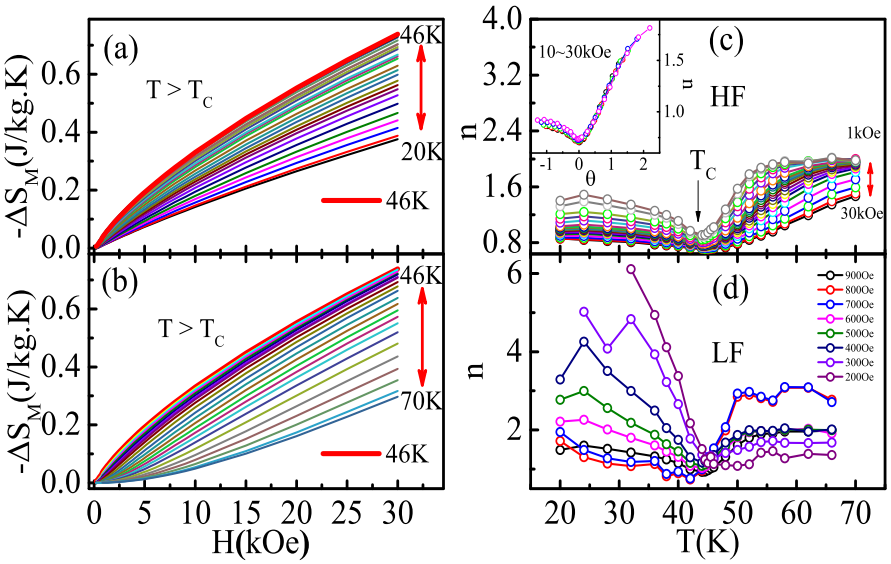

FIG. 5: (Color online) (a) and (b): Field dependent of $-\Delta S_M$ $[-\Delta S_M(H)]$ at different temperatures above and below T_C; (c) and (d): temperature dependence of n curves under high and low field (the inset of (c) shows the scaled n vs. θ for the curves under high field).

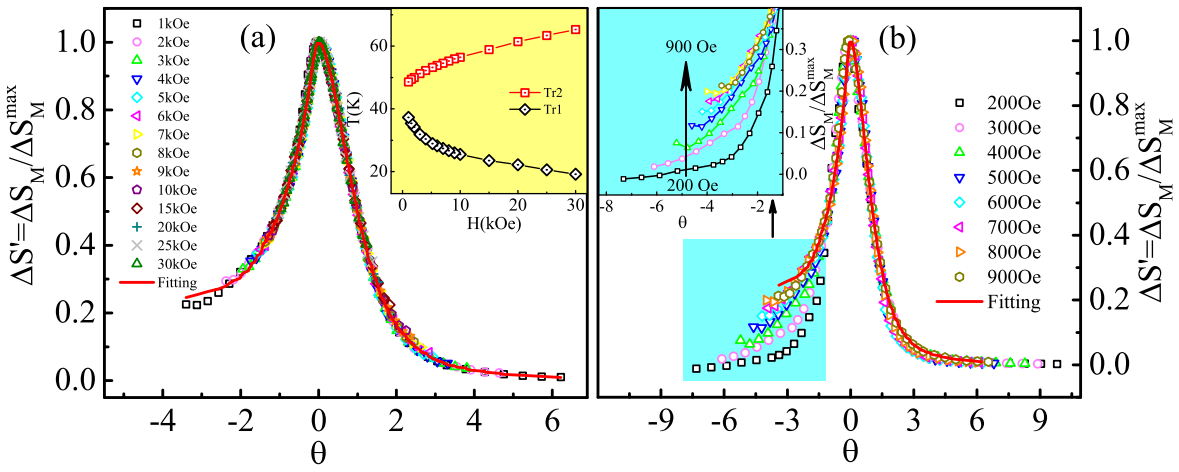

FIG. 6: (Color online) Scaling of the $-\Delta S_M(T,H)$ curves: (a) the normalized $\Delta S_M(T,H)$ as a function of scaled θ in high field region (the inset gives T_{r1} and T_{r2} as a function of H); (b) $\Delta S'_M(\theta)$ curves in low field region (the inset depicts the magnified region below T_C).